Latest results on heavy flavor di-lepton (p-Pb and Pb-Pb)

To cite this article: Dong Ho Moon and the CMS collaboration 2014 *J. Phys.: Conf. Ser.* **535** 012023

View the article online for updates and enhancements.

Related content

Latest results on heavy flavor di-lepton (p-Pb and Pb-Pb)

Dong Ho Moon on behalf of the CMS collaboration

University of Illinois at Chicago

E-mail: `dmoon@cern.ch`

Abstract. The Compact Muon Solenoid (CMS) has measured various quarkonium states via their decays into muon pairs in pp, PbPb and pPb collisions at $\sqrt{s_{NN}} = 2.76$ and 5.02 TeV. Quarkonia are especially relevant for studying the quark-gluon plasma since they are produced at early times of the collision and propagate through the medium, mapping its evolution. The most recent results on the production of prompt J/ψ in PbPb and the three Υ states in pp and pPb collisions will be presented.

1. Introduction

One strong signature of the existence for a Quark-Gluon-Plasma (QGP) is quarkonium suppression. Recent results from quarkonia measurements performed in CMS have been found to support theoretical predictions called the sequential melting scenario [1, 2, 3]. Quarkonimum production in heavy-ion collisions is affected by initial effects such as nuclear parton distribution functions (nPDFs) [4], parton energy loss, and the Cronin effect [5, 6], and final state effects such as Debye color screening and statistical recombination [1].

The result of study of the prompt J/ψ azimuthal anisotropy will be reported in this paper. Expected effects contributing to an observed non-zero elliptic anisotropy include recombination of thermalized charm quarks and (or) a path-length difference for absorption of quarkonia traversing the different direction of the almond-shaped hot and dense medium created in mid-central PbPb collisions.

This paper also reports the results of $b\bar{b}$ states produced in proton-lead (pPb) collisions. This system is a good reference to understand initial state effects and may allow insight into cold nuclear effects that differ from the suppression effects observed in previous measurements [7].

2. Environmental setup and analysis procedure

The central feature of the CMS apparatus is a superconducting solenoid, providing an axial magnetic field of 3.8 T. Immersed in the magnetic field are the silicon pixel and strip tracker, the lead-tungstate crystal electromagnetic calorimeter, and the brass/scintillator hadron calorimeter. Muons are measured in gas ionization detectors embedded in the steel return yoke and in the pseudorapidity window $|\eta| < 2.4$, with detection planes made of three technologies: Drift Tubes, Cathode Strip Chambers, and Resistive Plate Chambers. Matching the muons to the tracks measured in the silicon tracker results in a transverse momentum resolution better than 1.5% for p_T smaller than 100 GeV/c. A more detailed description of the CMS detector can be found in Ref. [8].
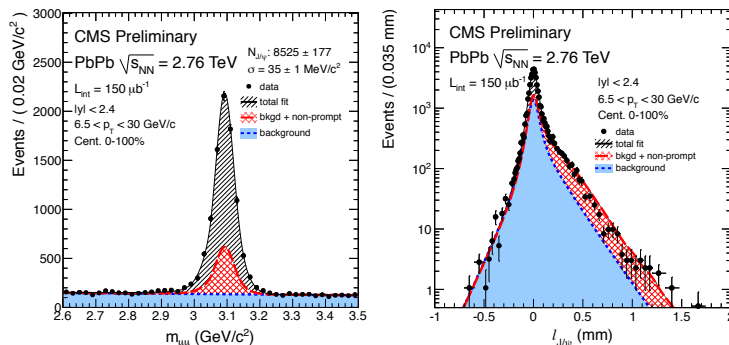
Figure 1. Invariant-mass spectra (left) and pseudo-proper decay length distribution (right) of $\mu^+\mu^-$ pairs integrated over centrality. The spectra are integrated over the rapidity range $0 < |y| < 2.4$ and the p_T range $6.5 < p_T < 30$ GeV/c. The projections of the two-dimensional fit onto the respective axes are overlaid as solid black lines. The dashed red lines show the fitted contribution of non-prompt J/ψ. The fitted background contributions are shown as dotted blue lines [9].
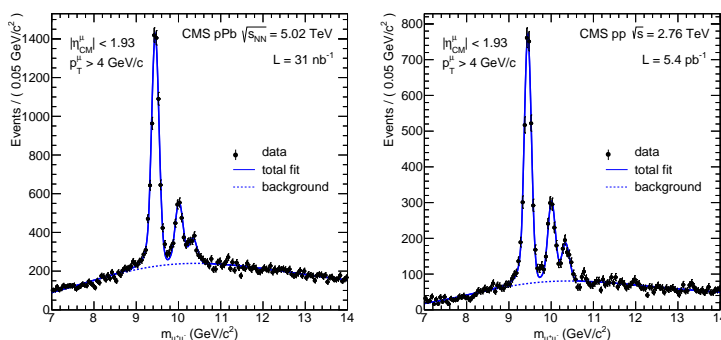

Figure 2. Invariant mass spectrum in pPb (left) and pp collisions (right) of $\mu^+\mu^-$ pairs with single muons with $p_T^\mu > 4$ GeV/c and $|\eta_{CM}^\mu| < 1.93$. The data (black circles) overlaid with the fit (solid blue line). The background component of the fit is represented by the dashed blue line [10].

The pp. data used in the study corresponded to an integrated luminosity of 5.4 pb^{-1} at a center-of-mass energy $\sqrt{s_{NN}} = 2.76$ TeV. The corresponding integrated luminosity of pPb data is 31 nb^{-1} with a center-of-mass energy $\sqrt{s_{NN}} = 5.02$ TeV. The direction of the higher-energy proton beam was initially set up to be clockwise, and was reversed after an integrated luminosity of 18 nb^{-1} of data was recorded. As a result of the energy difference of the colliding beams, the nucleon-nucleon center-of-mass in the pPb collisions are not at rest with respect to the laboratory frame. Massless particles emitted at $|\eta_{CM}| = 0$ in the nucleon-nucleon center-of-mass frame are detected at $\eta = -0.465$ (clockwise proton beam) or $+0.465$ (counterclockwise proton beam) in the laboratory frame. The PbPb data used for prompt J/ψ azimuthal anisotropy measurement were collected with a corresponding integrated luminosity of 150 μb^{-1}.

The invariant mass spectrum of all $\mu^+\mu^-$ pairs used in the PbPb analysis is shown in the left of Figure 1. The black curve is an extended unbinned maximum likelihood fit to the spectrum, using the sum of a Crystal Ball (CB) and a Gaussian function for signal, and an exponential for the background. To measure the fraction of non-prompt J/ψ (the so called b-fraction), the pseudo-proper decay length $l_{J/\psi}$, as shown in the right of Figure 1, is computed as an estimate

of the b-fraction decay length by $L_{xy} m_{J/\psi}/p_T$. Here, the L_{xy} is defined as,

$$L_{xy} = \frac{\hat{u}^T S^{-1} \vec{r}}{\hat{u}^T S^{-1} \hat{u}}, \tag{1}$$

where $\hat{u}$ is the unit vector in the direction of the J/ψ p_T and S is the sum of the primary and secondary vertex covariance matrices. In the final step, the invariant mass spectrum of $\mu^+\mu^-$ pairs and their $l_{J/\psi}$ distribution are fitted simultaneously in a two-dimensional (2D), extended unbinned maximum likelihood fit.

Figure 2 shows the mass spectra for Υ(nS) states in pp (left) and pPb (right). The yields are extracted from an unbinned maximum likelihood fit to the invariant dimuon mass spectra. The reconstructed mass line shape of each Υ(nS) state is modeled by a CB function, i.e. a Gaussian function with the low-side tail replaced by a power law function describing final-state radiation. Reasonable variations with multiplicity are considered in the systematic uncertainties. The Υ(nS) mass ratios are fixed to the their world average values [11], with ground shape is modeled by an exponential function multiplied by an error function and all its parameters are left free in the fit, as in Ref. [12].

3. Results
3.1. Charmonia in PbPb collisions
After extracting the prompt J/ψ yields in each rapidity, p_T, centrality, and $\Delta\phi$ bin, the v_2 is calculated with a fit of the $\frac{1}{N_{total}^{J/\psi}}\frac{dN_{J/\psi}}{d\phi}$ vs $\Delta\phi$ distributions with the function

$$1 + 2v_2\cos(2\Delta\phi). \tag{2}$$

The $N_{total}^{J/\psi}$ is the yield in $\Delta\phi = 2/\pi$ for each kinematic bin. An example of such fits is given in Figure 3, for the centrality integrated case. The measured prompt J/ψ v_2, for 10-60% event centrality, integrated over $6.5 < p_T < 30$ GeV/c and $|y| < 2.4$ is

$$0.054 \pm 0.013(\text{stat}) \pm 0.006(\text{syst}), \tag{3}$$

with a significance for a nonzero v_2 of 3.8σ. The v_2 results versus centrality, p_T, and rapidity are shown in Figure 4. For each of these results, the dependence on one variable is studied by averaging over the other two. A non-zero v_2 is measured in all the kinematic bins studied. The observed anisotropy shows no strong centrality or rapidity dependence when integrated over rapidity and centrality, respectively. In 10-60% centrality events, the result are compatible with a p_T-independent anisotropy, whether measured at low-p_T ($3 < p_T < 6.5$ GeV/c) in the forward rapidity interval $1.6 < |y| < 2.4$, or at high-p_T ($6.5 < p_T < 30$ GeV/c) in rapidity interval $|y| < 2.4$.

3.2. Bottomonia in pp and pPb collisions
The pp and pPb data are further analyzed separately as a function of event activity variables measured in two different rapidity regions. Specifically, the single ratios, Υ(2S)/Υ(1S) and Υ(3S)/Υ(1S) are measured in bins of: (1) $E_T^{|\eta|>4}$, the raw transverse energy deposited in the most forward part of the HF calorimeters at $4.0 < |\eta| < 5.2$, and (2) $N_{tracks}^{|\eta|<2.4}$, the number of charged particles, not including the two muons, with $p_T > 400$MeV/c reconstructed in the tracker at $|\eta| < 2.4$ and originating from the same vertex as the Υ. In Figure 5, for both pp and pPb, the results are shown as a function of forward transverse energy ($E_T^{|\eta|>4}$, left panel), and as a function of mid-rapidity track multiplicity ($N_{tracks}^{|\eta|<2.4}$, right panel). The difference observed
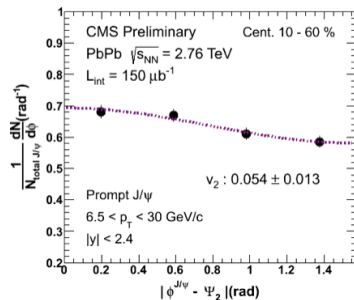
Figure 3. The $\Delta\phi$ distribution of high-p_T ($6.5 < p_T < 30$ GeV/c) prompt J/ψ raw yields, measured in the rapidity range $|y| < 2.4$ and event centrality 10-50%, and normalized by the bin width and the sum of the yields in all four $\Delta\phi$ bins. The dashed red line in all figures represents the function $1+2v_2\cos(2\Delta\phi)$ used to extract v_2 [9].
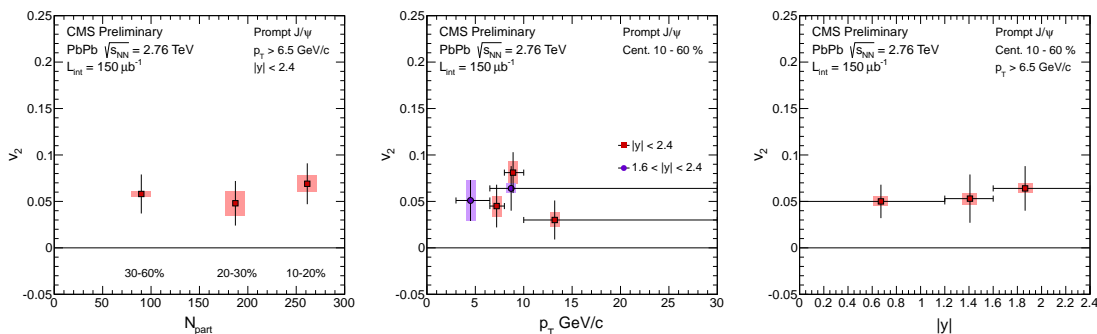

Figure 4. Prompt J/ψ centrality (left), p_T (middle) and rapidity (right) dependence of v_2. The boxes represented point-by-point systematic uncertainties. Horizontal bars indicate the bin width [9].

between the Υ states when binning in $N_{tracks}^{|\eta|<2.4}$ can be explained in two opposite ways. If, on one hand, the Υ(1S) is systematically produced with more particles than the excited states, it would influence the underlying distribution of charged particles and create an artificial effect when selected in small multiplicity bins. This effect should be sensitive to the underlying multiplicity distribution and would result in a larger correlation if one reduces the size of the multiplicity bins. On the other hand, if the Υ are interacting with the surrounding environment, the Υ(1S) is expected, as the most tightly bound state and the one of smallest size, to be less affected than Υ(2S) and Υ(3S), leading to a decrease of the Υ(nS)/Υ(1S) ratios with increasing multiplicity. In either cases, the ratios will continuously decrease from the pp to pPb to PbPb systems, as a function of event multiplicity.

In addition, self-normalized to their activity-integrated values, the individual Υ(nS) yields are calculated. The results are shown in Figure 6 in bins of $E_T^{|\eta|>4}/\langle E_T^{|\eta|>4}\rangle$ (top) and $N_{tracks}^{|\eta|<2.4}/\langle N_{tracks}^{|\eta|<2.4}\rangle$ (bottom), for pp and pPb collisions, where the denominator is average of yields in all events. All the self-normalized cross section ratios increase with increasing forward transverse energy and mid-rapidity particle multiplicity in the event. In the cases where Pb ions are involved, the increase observed in both variables can arise from the increase in the number of nucleon-nucleon collisions. The pp results are reminiscent of a similar J/ψ measurement made in pp collisions at 7 TeV [13].
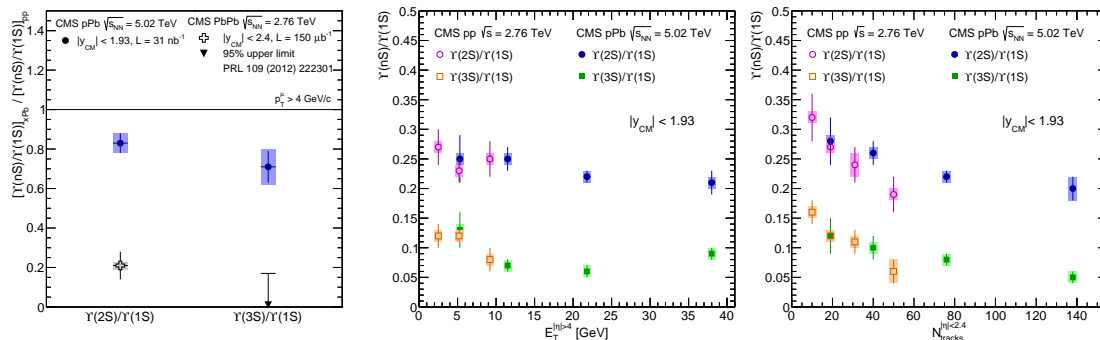
Figure 5. (Left) Event activity integrated double ratios of the excited states, $\Upsilon(2S)$ and $\Upsilon(3S)$, to the ground state, $\Upsilon(1S)$ in pPb collisions at $\sqrt{s_{NN}} = 5.02$ TeV with respect to pp collisions at $\sqrt{s} = 2.76$ TeV (circles), compared to the corresponding ratios for PbPb (cross) collisions at $\sqrt{s_{NN}} = 2.76$ TeV from Ref. [12], which used a different dataset for the pp normalization. (Middle, Right) Single cross section ratios $\Upsilon(2S)/\Upsilon(1S)$ and $\Upsilon(3S)/\Upsilon(1S)$ for $|y_{CM}| < 1.93$ versus transverse energy measured in $4.0 < |\eta| < 5.2$ (left) and number of charged tracks measured in $|\eta| < 2.4$ (right), for pp collisions at $\sqrt{s} = 2.76$ TeV (open symbols) and pPb collisions at $\sqrt{s_{NN}} = 5.02$ TeV (closed symbols). In both figures, the error bars indicate the statistical uncertainties, and the boxes represent the point-to-point systematic uncertainties. The global uncertainties on the pp results are 7% and 8% for $\Upsilon(2S)/\Upsilon(1S)$ and $\Upsilon(3S)/\Upsilon(1S)$, respectively, while in the pPb results they amount to 8% and 9%, respectively [10].

4. Summary

We presented the azimuthal anisotropy of prompt J/ψ that shows a 3.8σ significance for a non-zero v_2 in the centrality 10-60% of high p_T (>6.5 GeV/c) over rapidity range $|y| < 2.4$. No strong centrality, p_T and rapidity dependence is observed within the measured uncertainties for results that integrate the other variables. This result could give a hint of the path-length dependence of partonic energy loss in a deconfined medium.

The results of double ratios $[\Upsilon(nS)]/[\Upsilon(1S)]_{pPb}/[\Upsilon(nS)]/[\Upsilon(1S)]_{pp}$ suggests the presence of final-state suppression effects in the pPb collisions compared to pp collisions which affect more strongly the excited states ($\Upsilon(2S)$ and $\Upsilon(3S)$) compared to the ground state ($\Upsilon(1S)$). The excited-to-ground-states cross section ratios, $\Upsilon(nS)/\Upsilon(1S)$, are found to decrease with increasing charged-particle multiplicity as measured in the $|\eta| < 2.4$ interval that contains the region in which the Υ are measured. The self-normalized cross section ratios, $\Upsilon(nS)/\langle\Upsilon(nS)\rangle$ increase with event activity.

References
[1] T. Matsui and H. Satz, *Phys. Lett. B* **178** (1986) 416
[2] S. Digal, P. Petreczky, and H. Satz, *Phys. Rev. C* **64** (2001) 904015
[3] A. Mocsy and P. Petreczky, *Phys. Rev. Lett* **99** (2007) 211602
[4] R. Vogt, *Phys. Rev. C* **81** (2010) 044903
[5] R. Sharma and I. Vitev, *Phys. Rev. C* **87** (2013) 044905
[6] F. Arleo and S. Peigne, *JHEP* **03** (2013) 122
[7] CMS Collaboration, *JHEP* **1205** (2012) 063
[8] CMS Collaboration, *JINST* **3** (2008) S08004
[9] CMS Collaboration, CMS Physics Analysis Summary CMS-HIN-12-001 (2012)
[10] CMS Collaboration, *JHEP* **04** (2014) 103
[11] Particle Data Group Collaboration *Phys. Rev. D* **86** (2012) 010001
[12] CMS Collaboration, *Phys. Rev. Lett.* **109** (2012) 222301
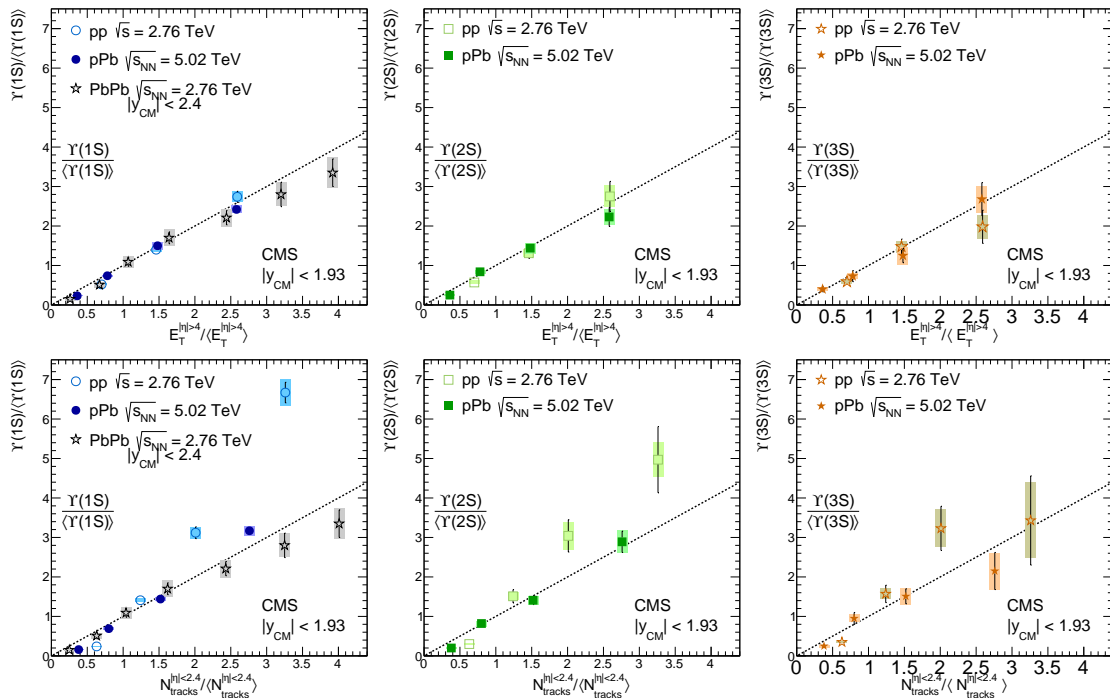[13] ALICE Collaboration, *Phys. Rev. Lett. B* **712** (2012) 165

Figure 6. The $\Upsilon(nS)$ cross section versus transverse energy measured at $4 < |\eta| < 5.2$ (top row) and versus charged-track multiplicity measured in $|\eta| < 2.4$ (bottom row), measured in $|y_{CM}| < 1.93$ in pp collisions at $\sqrt{s} = 2.76$ TeV and pPb collisions at $\sqrt{s_{NN}} = 5.02$ TeV. For $\Upsilon(1S)$, the PbPb data at $\sqrt{s_{NN}} = 2.76$ TeV (open stars) are overlaid. Cross sections and x-axis variables are normalized by their corresponding activity-integrated values. For all points, the abscissae are at the mean value in each bin. The dotted line is a linear function with a slope equal to unity. The error bars indicate the statistical uncertainties, and the boxes represent the point-to-point systematics uncertainties [10].